# p63 supports aerobic respiration through hexokinase II

Guiditta Viticchiè[a], Massimiliano Agostini[a,b], Anna Maria Lena[a], Mara Mancini[a,b], Huiqing Zhou[c], Lello Zolla[d], David Dinsdale[b], Gaelle Saintigny[e], Gerry Melino[a,b,1], and Eleonora Candi[a,f,1]

[a]Department of Experimental Medicine and Surgery, University of "Tor Vergata", 00133 Rome, Italy; [b]Toxicology Unit, Medical Research Council, Leicester LE1 9HN, United Kingdom; [c]Department of Molecular Developmental Biology, Radboud University, 6525 GA Nijmegen, The Netherlands; [d]Department of Ecological and Biological Sciences, Tuscia University, 01100 Viterbo, Italy; [e]Chanel Parfumes Beauté, F-92521 Neuilly-sur-Seine, France; and [f]Istituto Dermopatico dell'Immacolata, Istituto di Ricovero e Cura a Carattere Scientifico, 00167 Rome, Italy

Edited by Tak W. Mak, The Campbell Family Institute for Breast Cancer Research at Princess Margaret Cancer Centre, University Health Network, Toronto, ON, Canada, and approved August 6, 2015 (received for review May 6, 2015)

**Short p63 isoform, ΔNp63, is crucial for epidermis formation, and it plays a pivotal role in controlling the turnover of basal keratinocytes by regulating the expression of a subset of genes involved in cell cycle and cell adhesion programs. The glycolytic enzyme hexokinase 2 (HK2) represents the first step of glucose utilization in cells. The family of HKs has four isoforms that differ mainly in their tissue and subcellular distribution. The preferential mitochondrial localization of HK2 at voltage-dependent anion channels provides access to ATP generated by oxidative phosphorylation and generates an ADP/ATP recycling mechanism to maintain high respiration rates and low electron leak. Here, we report that ΔNp63 depletion in human keratinocytes impairs mitochondrial basal respiration and increases mitochondrial membrane polarization and intracellular reactive oxygen species. We show ΔNp63-dependent regulation of HK2 expression, and we use ChIP, validated by p63-Chip sequencing genomewide profiling analysis, and luciferase assays to demonstrate the presence of one p63-specific responsive element within the 15th intronic region of the HK2 gene, providing evidence of a direct interaction. Our data support the notion of ΔNp63 as a master regulator in epithelial cells of a combined subset of molecular mechanisms, including cellular energy metabolism and respiration. The ΔNp63–HK2 axis is also present in epithelial cancer cells, suggesting that ΔNp63 could participate in cancer metabolic reprogramming.**

p63 | HK2 | keratinocytes | oxidative metabolism | mitochondria

The epidermis is a multilayer epithelium that continuously renews during the organism lifespan. The continuous maintenance and homeostasis of this tissue in adult life reflects the embryonic process. Indeed, specific cells of the basal layer escape upward to the outer surface during the process of terminal differentiation (1). These cells, also defined as transient amplifying (TA) cells, display a limited proliferative potential. The expression of protein markers that favor migration to the differentiation compartments, the spinous and granular layers, and finally the cornified envelope, begins after a few cell divisions (2–4). The cells undergoing terminal differentiation are replaced by the cells of the basal layer that will become new TA cells, maintaining a balance between differentiation and proliferation (1, 4). In this context, the transcription factor p63 plays a crucial role in regulating the turnover of basal keratinocytes in developing and adult epidermis (5–8). Indeed, $p63^{-/-}$ mice completely lack epidermis and epidermal derivatives and die within a few hours after birth (9, 10). TP63 gene is transcribed by two different promoters, giving rise to the longer isoform, TAp63, which includes the transactivation domain, and the short isoform, ΔNp63, which lacks the N-terminal transactivation domain (11, 12) but is still transcriptionally active because of a second C-terminal transactivation domain (13, 14). $\Delta Np63^{-/-}$ mice recapitulate the epithelial and developmental defects described in the full $p63^{-/-}$ mice, demonstrating that ΔNp63 is the crucial isoform for epithelial systems, including the epidermis (15). Although strong evidence demonstrates the important role of ΔNp63 in maintaining the proliferative potential of epithelial cells (16), we are aware of no investigations that have probed the importance of ΔNp63 in energy metabolism in cells with a high proliferative potential, conversely, to the TAp63 isoform (17).

Aiming to expand our knowledge of ΔNp63 and cell metabolism in human keratinocytes, we found that hexokinase (HK) 2 (HK2), but not HK1, is strongly depleted in the absence of p63 and that a specific p63-binding motif is localized within the 15th intronic region of the HK2 genomic sequence, working as an enhancer. We demonstrate that HK2 is a p63 direct target gene acting as a downstream regulator of mitochondrial reactive oxygen species (ROS) generation. The p63–HK2 axis significantly enhances the coupling between glucose metabolism and oxidative phosphorylation, providing the energy to sustain cell proliferation and protecting cells from oxidative stress.

## Results

**p63 Silencing Induces Mitochondrial Oxidative Stress with Mitochondrial Membrane Hyperpolarization.** To determine the effect of p63 depletion in human primary keratinocytes (Hekn cells), siRNA for p63 was transfected, and the phenotypic effects were evaluated at 48 h. The analysis of the chloromethyl derivate of 2′,7′-dichlorodihydrofluorescein diacetate (CM-$H_2$DCFDA) revealed an increased intracellular hydrogen peroxide content of ∼20% (Fig. 1*A*). Furthermore, p63 silencing reduced the expression of genes such as glutathione peroxidase (GPX) 2, mitochondrial superoxide dismutase (SOD2), and NADPH quinone oxidoreductase (NQO1; Fig. 1*B*), in keeping with oxidative stress. MitoSOX Red staining showed a 40% increase in the mitochondrial superoxide anion content (Fig. 1*C*) without changes in the mitochondrial mass (probed with MitoTracker Green staining) or in mitochondrial biogenesis (probed by analyzing the expression of the mitochondrial gene Nd1; Fig. S1*A*). EM showed normal mitochondrial morphology and no significant variation in the number of organelles (Fig. S1*B*). Consistently, the

### Significance

**The importance of ΔNp63 in controlling metabolism has not been investigated so far. We identified a regulatory pathway involving ΔNp63 and the glycolytic enzyme hexokinase 2 (HK2). ΔNp63 direct-dependent regulation of HK2 expression contributes to the coupling between glucose metabolism and oxidative phosphorylation, providing the energy necessary to sustain cell proliferation and protecting cells from oxidative stress. The ΔNp63–HK2axis is also present in epithelial cancer cells, suggesting that ΔNp63 could participate in cancer metabolic reprogramming.**

Author contributions: G.M. and E.C. designed research; G.V., M.A., A.M.L., M.M., L.Z., and D.D. performed research; A.M.L., H.Z., and G.S. contributed new reagents/analytic tools; G.V. analyzed data; and G.V., G.M., and E.C. wrote the paper.

The authors declare no conflict of interest.

This article is a PNAS Direct Submission.

[1]To whom correspondence may be addressed. Email: candi@uniroma2.it or gm89@le.ac.uk.

This article contains supporting information online at www.pnas.org/lookup/suppl/doi:10.1073/pnas.1508871112/-/DCSupplemental.

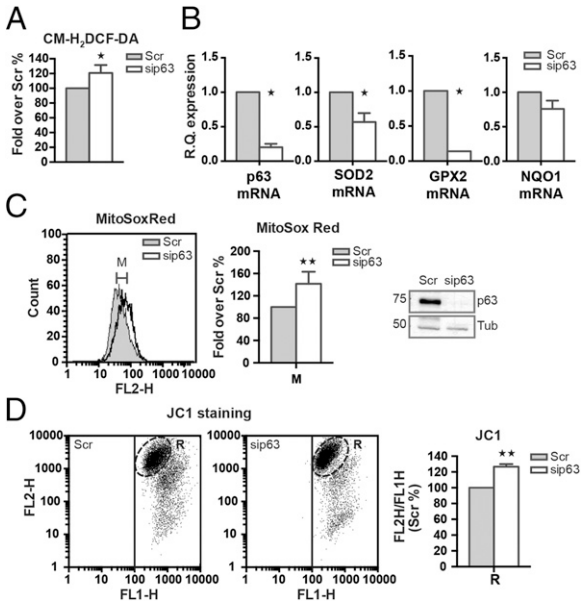


**Fig. 1.** siRNA-mediated p63 silencing induces mitochondrial oxidative stress and increases mitochondrial membrane polarization. (*A*) To determine the intracellular $H_2O_2$ level, 10 μM CM-$H_2$DCFDA was used 48 h after transfection. The histogram shows the relative quantification of the emission signal of the fluorescein probe compared with the control (Scr; siRNA). (*B*) mRNA expression by real-time quantitative PCR (qPCR) of oxidative stress genes: mitochondrial SOD2, GPX2, and NQO1. p63 mRNA is shown as a transfection control. (*C*) MitoSOX Red analysis by flow cytometry was performed 48 h after p63 depletion to assay mitochondrial superoxide anion levels (*Left*), and the increase in fluorescence intensity (labeled "M") was quantified as shown in the histogram. The Western blot (*Right*) shows p63 silencing efficiency at the protein level. Tubulin was used as a loading control. (*D*) FACS analysis of JC1 staining was performed under the same conditions of MitoSOX Red and CM-$H_2$DCFDA (48 h after transfection) to determine changes in the mitochondrial membrane polarization. The upper right quadrants of the dot plots collect cells positive for mitochondrial JC1 aggregates related to polarized mitochondria. The red fluorescence signal decrease correlates with JC1 monomer accumulation in the cytoplasmic compartment corresponding to depolarized mitochondria. Gate R was assessed to analyze highly polarized mitochondria, and the histogram (*Right*) is the relative quantification of JC1 spectral emissions (FL2-H/FL1-H ratio). The FACS results are shown as the mean ± SD from three independent experiments. All data are shown as the mean ± SD from three independent experiments (**P* < 0.01 and **P* < 0.001).

protein steady-state level of the electron transport chain complexes was not affected by p63 depletion (Fig. S1*C*), but a 25% increase in the mitochondrial membrane polarization was observed (demonstrated with J-aggregate-forming delocalized lipophilic cation (JC1) staining; Fig. 1*D*).

**p63 Depletion Reduces Oxygen Consumption and Unbalances Energetic Demand Through the Glycolytic Pathway.** We then evaluated oxidative metabolism, keeping in mind that p53 regulates aerobic respiration through several pathways (18, 19). We found that p63-depleted cells had a significantly reduced oxygen consumption rate (OCR; Fig. 2*A*). As shown in Fig. 2*A*, the OCR profile of sip63 samples was similar to the control, supporting the idea that mitochondria retain sensitivity to environmental stress. However, the relative quantification of OCR corresponding to the single stages of the analysis showed an inability to rely on aerobic respiration (histogram in Fig. 2*A*). As shown in Fig. 2*B*, oligomycin injection induced anaerobic metabolism in the control cells, as observed by the increased extracellular acidification rate (ECAR). Although sip63 cells showed a similar response pattern, leading to an increase of ECAR from the basal respiration (BR) stage to the uncoupling respiration (UR) stage (Fig. S2*A*), they failed to rescue the control cells that were unable to rely on the glycolytic pathway. To further investigate this finding, we performed a metabolomic profile of glycolytic intermediates through gas and liquid chromatography/MS (Fig. 2*C* and Fig. S2*B*). The glucose concentration doubled 48 h after transfection (Fig. 2*C*). Importantly, the intracellular ADP level was significantly increased, and the production of lactate was not enhanced, whereas other biochemicals (phosphoenolpyruvate, glucose-6-phosphate, fructose-6-phosphate) significantly increased (Fig. S2*B*). We correlated this result with the ECAR measurements, supporting the idea of the inability of p63-depleted cells to redirect metabolism. Finally, the reduction of intracellular ATP confirmed this hypothesis (Fig. 2*C*, *Right*).

**HK2 Is a p63 Direct Target Gene.** To find a molecular mediator downstream of p63 that supports mitochondrial function, we examined the expression of a large cohort of mitochondrial genes. As shown in Figs. 1*B* and 3*A*, we observed that the transcription of most of the GPXs was strongly affected and that the expression of cytochrome *c* oxidase synthase and cyclooxygenase 2, also known as prostaglandin-endoperoxide synthase, were impaired by p63 knockdown. Surprisingly, of the two main regulators of glycolysis, HK1 and HK2, only HK2 mRNA was strongly down-regulated (Fig. 3*B*). The

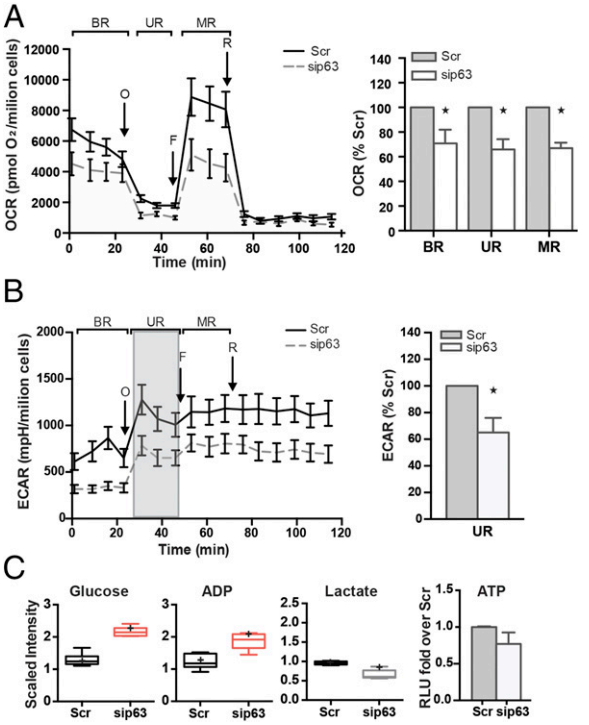


**Fig. 2.** p63-depleted keratinocytes display deficiency in mitochondrial oxygen consumption and inability to balance energetic demand through the glycolytic pathway. OCR (*A*) and ECAR (*B*) performed in 24-well Seahorse assay plates show the cellular respiration profile after treatment with the drugs oligomycin ("O," 0.5 μM), FCCP ("F," 0.4 μM), and rotenone ("R," 1 μM). The curves (*A* and *B*, *Left*) are representative of three independent experiments, each expressed as the mean ± SD normalized to the cell number. The relative quantification of the area below the curves corresponding to the stages labeled with BR, UR, and MR are shown in histograms (*A* and *B*, *Right*). (*C*) Metabolic profile of the glycolytic pathway was carried out by Metabolon as described in *SI Materials and Methods*. The values for each metabolite are normalized to the protein content, and the average of the distribution is represented by the cross symbol within the box. Statistical significance was assessed by Welch *t* tests, and red boxes are representative of $P < 0.05$ (asterisk). The ATP levels of Hekn cells after 48 h of siRNA transfection were normalized to the cell number and are reported as relative quantification to the Scramble transfected sample (**P* < 0.05). The Western blot shows the efficiency of transfection displaying tubulin as a loading control.

80% HK2 transcriptional repression was consistent with a reduced amount of the steady-state protein level (Fig. 3*B*). HK2 contains a mitochondria-targeting domain that allows the interaction of the cytoplasmic enzyme with the voltage-dependent anion channel (VDAC)/adenine nucleotide translocase channel.

Based on the previous results, we investigated whether HK2 could be a p63 direct target gene. Molecular analysis showed two p53 responsive elements in the HK2 promoter (Fig. 3*C*), and a previous report demonstrated that a sequence from the rat HK2 promoter could be controlled by p53 (20). A sequence of ∼1,200 bp upstream of the transcription start site that contained the p53 responsive elements (REs) I and II was cloned into a pGL3-promoter vector containing the luciferase reporter gene. In our experimental set, neither p53 nor p63 transactivated the human promoter (Fig. 3*D*), but a further investigation of the genomic sequence, taking advantage of the genomewide p63 ChIP-Seq profiles in human keratinocytes from a previous study (21, 22), noted a specific p63 binding element in the 15th intronic region of the genomic sequence (Fig. 3*C* and Fig. S3*A*). This p63 binding element seemed to be an active enhancer, as it is colocalized with the active enhancer mark H3K27ac (Fig. S3*A*).

Luciferase assay analysis of ∼600 nt of the related sequence (REIII) showed that p63 enhances the luciferase activity by ∼18 fold, whereas p53 showed a lower, fivefold enhancement and transactivating function (Fig. 3*D* and Fig. S4). Finally, REIII-specific mutagenesis abolished luciferase activity, demonstrating the specificity of the sequence. Next, to validate the result of the ChIP-Seq, we performed a ChIP assay in our cells and demonstrated a physical interaction between p63 and the HK2 intronic region (Fig. 3*E*). To verify if ΔNp63 contributed to HK2 transcription in epithelial cancer cells, we repeated selected experiments by using the breast cancer cell line HCC1937, which expresses ΔNp63 at high level. First, we observed that, in HCC1937 cells, p63 knockdown strongly reduced HK2 at the mRNA (55% reduction) and protein levels (Fig. S5 *A* and *B*). Second, we demonstrated by ChIP that ΔNp63 specifically binds this previously unidentified intronic enhancer (Fig. S5*C*), with the MTSS1 gene used as positive control (23). These data clearly demonstrated that ΔNp63, binding the identified enhancer, significantly contributes to HK2 transcription in human keratinocytes and in the HCC1937 breast cancer cell line.

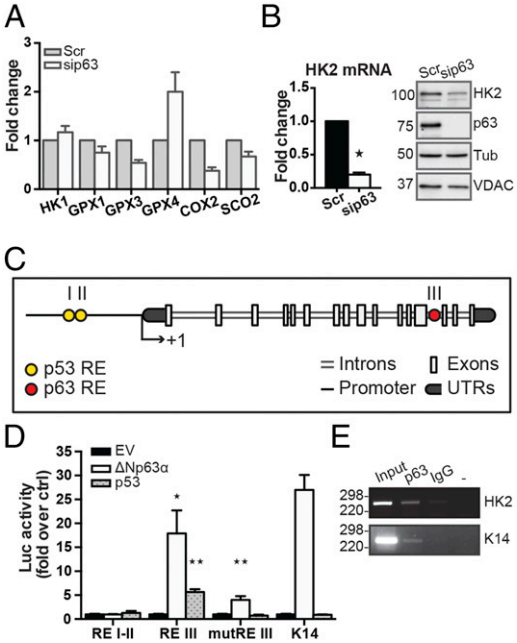


**Fig. 3.** HK2 is a p63 direct target gene. Real-time qPCR of oxidative stress genes (*A*) and HK2 mRNA (*B*) was performed after 48 h of sip63 transfection in human keratinocytes. The data are representative of three independent measurements and consistent with an 80% decrease of HK2 transcription (*$P < 0.01$). Western blot was carried out to assess HK2 protein level in the same conditions. VDAC and tubulin are shown as mitochondrial and cytoplasmic loading controls, respectively. (*C*) The HK2 gene structure shows the presence of a putative p63 responsive element (i.e., REIII) in the 15th intron of the genomic sequence. (*D*) Luciferase assay shows ΔNp63α-meditated transactivation of REIII of HK2 gene in 293E cells. The sequences corresponding to REI, REII, REIII and REIII mutant counterparts were inserted into a Luc reporter-containing pGL3 promoter vector, and the selectivity of the transactivation was tested by using constructs for ΔNp63α and p53. The K14 promoter was used as a positive control. Luc activity was assessed as the mean ± SD of three independent experiments (*$P < 0.05$ and **$P < 0.01$). (*E*) ChIP analysis performed in Hekn shows physical binding of the ΔNp63α transcription factor to the HK2 intronic region REIII. ChIP on the K14 promoter was used as a positive control.

**HK2 Knockdown Phenocopies p63 Silencing.** To explore the biological relevance of the p63–HK2 axis sustaining oxidative metabolism in human keratinocytes, we sought to verify whether HK2 silencing could phenocopy the biological effects of p63 silencing. Indeed, HK2 silencing, as shown by the OCR and ECAR profiles, resembled the patterns of p63 silencing (Fig. 4*A*). Interestingly, the extent of mitochondrial impairment was similar in both treatments, demonstrating the crucial role of the glycolytic enzyme HK2 in metabolic effects mediated by p63. The mitochondrial superoxide anion level was strongly increased, and JC1 staining indicated a higher polarization of the mitochondrial membrane compared with the control (Fig. 4*B*). Finally, HK2 silencing reduced 5-ethynyl-2′-deoxyuridine (EdU) incorporation, leading to an approximate 40% reduction of cell proliferation (Fig. 4*C*). This observation is consistent with a previous report that p63 inhibited the proliferative capacity of basal keratinocytes and induced the arrest of the cell cycle in G1 phase (24). Furthermore, the colony formation capacity was strongly impaired (Fig. 4*C*). All together, these results highlight the importance of the aforementioned p63–HK2 axis as a branch of the orchestrated program through which p63 regulates cell metabolism and proliferation in human keratinocytes. Although cancer cells present mitochondria dysfunction and reduction in mitochondrial respiration capacities as a result of metabolic reprogramming, we found an effect upon HK2 knockdown in HCC1937 (Fig. S5 *D*–*F*) in terms of JC1 staining, indicating that, similarly to p63, siHK2 results in a higher polarization of the mitochondrial membrane compared with the control (Fig. S5 *E* and *F*).

Finally, we investigated the possibility for cross-talk between p53 and the HK1 isoform in the p63–HK2 axis in keratinocytes. p53 silencing after 48 h of transfection did not affect mitochondrial function, and no evidence of increased ROS production and membrane polarization were observed (Fig. S6). Furthermore, p53 depletion did not compromise cell proliferation, suggesting that basal keratinocytes rely mainly on p63 function for the regulation of proliferation and differentiation, whereas they activate p53 only in response to external injury and damage (e.g., UV damage). Finally, we found that p63 silencing did not affect HK1 expression at the mRNA and protein levels (Fig. 3*A* and Fig. S6*D*), excluding the possibility of a direct interaction between p63 and other HK variants. Consistently, HK1 depletion reduced the mitochondrial oxygen consumption capacity to a lower extent compared with HK2 silencing and, strikingly, did not affect the ability of human keratinocytes to redirect the metabolic program to the glycolytic pathway (Fig. S6*A*). These findings suggest that, in the absence of HK1, HK2 can compensate for the cellular defects. The reduction of cell proliferation in siHK1 cells was ascribed to the inversion of the metabolism from the high ATP yield of mitochondrial respiration to the low ATP yield of the anaerobic pathway. Finally, the observation that the mitochondrial ROS after HK1 depletion did not mirror the increased oxidative stress seen in HK2-depleted

CELL BIOLOGY

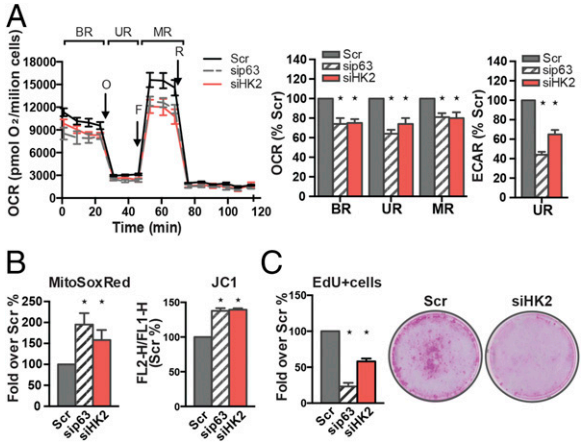


**Fig. 4.** Human keratinocytes silenced for HK2 phenocopy p63-depleted cells. (*A*) Real-time measurements (mean ± SEM; $n = 3$; $^*P < 0.01$) of OCR were performed as in Fig. 2 after 48 h of p63 and HK2 silencing (*Left*). The relative quantification of OCR and ECAR evaluated as percentage of control (Scr) are displayed in histograms (*Middle* and *Right*). (*B*) MitoSOX Red and JC1 staining confirm the similarities between sip63 and siHK2 phenotypes. Silencing HK2 in Hekn resembles the increase of superoxide anion levels and mitochondrial membrane polarization observed in p63-depleted cells (mean ± SD; $n = 3$; $^*P < 0.01$). (*C*) HK2-depleted keratinocytes display reduced proliferative potential. EdU staining by flow cytometry demonstrates a 50% reduction of proliferation 48 h after Hekn transfection (*Left*). A clonogenic assay that transfected human keratinocytes with the Scramble control and siHK2 confirms a reduction in colony formation after 12 d of culture. The micrographs shown are representative images of one of three independent experiments.

cells led us to conclude that proliferating keratinocytes rely on the p63–HK2 axis to sustain mitochondrial oxidative metabolism.

**Overexpression of HK2 cDNA Protects Human Keratinocytes from the Mitochondrial Dysfunction Induced by p63 Depletion.** To quantify the HK2 dependency of this p63 function, we decided to restore HK2 protein levels in p63-depleted keratinocytes to evaluate a possible rescue of the mitochondrial impairment. Viral ectopic expression of HA-HK2 cDNA almost restored the rate of oxygen consumption to the control values (Fig. 5 *A*–*C*). In detail, we observed a significant partial recovery of BR, probably because of the destabilization induced by the absence of p63, but we found that, after oligomycin injection, HK2 fulfilled the role of a metabolic inverter, enhancing the rate of acidification of the medium. In addition to this observation, in HK2-supplemented cells, after carbonyl cyanide p-trifluoro-methoxyphenyl hydrazone (FCCP) injection, the spare respiratory capacity was restored to normal levels, underlining the contribution of HK2 in helping mitochondria to perform electron transport at the maximal rate. Furthermore, we measured a strong decrease in mitochondrial superoxide anion production (Fig. 5*B*), suggesting that mitochondrial ROS are upstream effectors of mitochondrial impairment and related side effects. Proliferation was not rescued by HK2 reintroduction, as indicated by phospho-H3 Western blot (Fig. 5*C*), indicating that keratinocytes rely mainly on p63 function for proliferation.

We reported earlier that p63 regulates a subset of oxidative stress genes such as mitochondrial SOD2. Importantly, this enzyme is responsible for the dismutation of the superoxide anion in oxygen and hydrogen peroxide. Because we observed a reduction of the superoxide anion levels, in the context of reduced expression of SOD2 after HK2 restoration, we postulate that the recovery of mitochondrial activity is the crucial factor preventing secondary superoxide anion formation. Finally, the data presented here elucidate a mechanism through which HK2 acts as a p63 downstream target gene in sustaining proliferating keratinocytes (Fig. 5*D*). Of note, we proposed that p63 displays its role of master regulator involving the recruitment of a metabolic enzyme whose function is to enhance the coupling between glucose metabolism and mitochondrial function.

## Discussion

In the present study, we used primary keratinocytes as an experimental model to describe a ΔNp63-dependent regulatory mechanism of cell metabolism supporting epithelial proliferation. We found that, in the absence of ΔNp63, which is the most abundant p63 isoform in proliferating epithelial cells, keratinocytes undergo oxidative stress and mitochondrial dysfunction. In an attempt to investigate the direct ΔNp63 regulation of mitochondrial activity, we found out that HK2, one of the key regulators of glycolysis, is transcriptionally activated by ΔNp63. In addition, the ΔNp63–HK2 axis is responsible for the coupling of glucose metabolism and mitochondrial respiration (Fig. 5*D*). Specifically, in proliferating

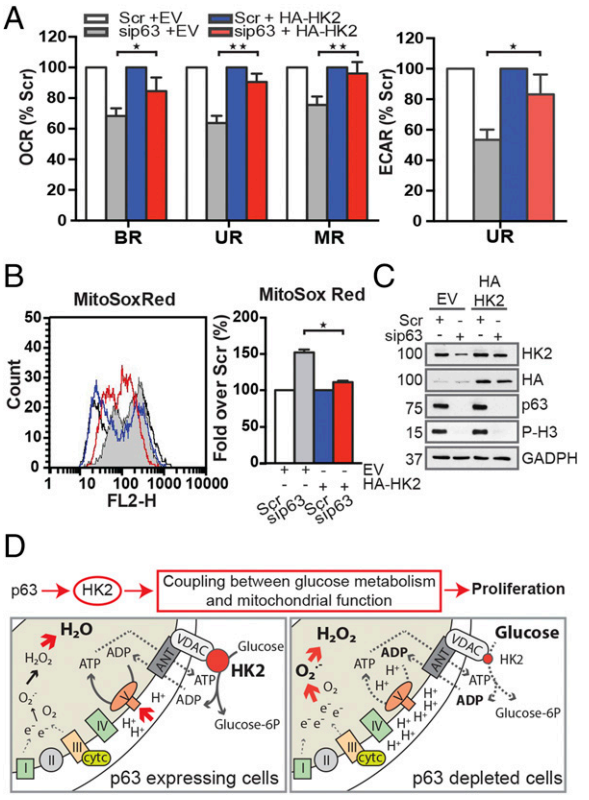


**Fig. 5.** Overexpression of HK2 cDNA protects human keratinocytes from mitochondrial dysfunction induced by p63 depletion. After 24 h of sip63 transfection, HK2 cDNA was introduced into human keratinocytes by retrovirus infection. (*A*) OCR and ECAR (mean ± SEM; $n = 3$) measurements after 48 h of viral infection. Histograms show the relative quantification corresponding to the different stages of cellular respiration (BR, UR, and MR) related to the injection of the drugs ("O," "F," "R"), as described in Fig. 2 ($^*P < 0.05$ and $^{**}P < 0.01$). (*B*) The MitoSOX Red profile (*Left*) shows fluorescence emission collected in the FL2-H channel after 48 h of viral infection. Relative quantification is presented in a histogram (*Right*) as described in Fig. 1 ($^*P < 0.01$). (*C*) Protein lysates were collected to verify viral infection of Hekn cells. Western blots show the rescue of HK2 protein levels in p63-depleted keratinocytes after expression of the HA-HK2 cDNA construct. The exogenous protein was detected by using anti-HA antibodies, whereas HK2 knockdown was confirmed by using anti-HK2 antibodies. Proliferation was evaluated by using anti–phospho-H3 staining. GADPH was used as a loading control. (*D*) A schematic summary representing the biological effects of the p63–HK2 axis in human keratinocytes. p63 sustains the proliferative state of basal cells partially through the coupling of glucose metabolism and mitochondrial function. (*Lower*) Detailed model of the mitochondrial state in the presence or absence of p63.

cells, HK2 silencing resembles the phenotype displayed by ΔNp63 depletion, and the restoration of HK2 protein levels in the absence of p63 is sufficient to revert the mitochondrial impairment to normal conditions. Our genomewide analysis confirmed the ChIP results, showing that p63 is physically bound to a previously unidentified p63-responsive element located in the 15th intron of the HK2 sequence. Through this element, p63 positively regulates HK2 transcription, indicating that this region acts as an enhancer regulatory element.

HKs control the first step of glycolysis, catalyzing the ATP-dependent phosphorylation of glucose to generate glucose-6-phosphate (25). In mammals, the family of HKs comprises four main isoforms differing in their substrate affinity, the inhibition induced by the product, their tissue expression, and their intracellular localization (26). HK1 and HK2 are high-affinity isoforms associated with mitochondria, and, whereas the former is constitutively expressed in most adult tissues, the latter is abundantly detected in adipose, cardiac, and skeletal muscle (27, 28). Similarly, HK3 is a high-affinity isoform, but it is inhibited by physiological concentrations of glucose (25). Finally, HK4, also known as glucokinase, has a low affinity for glucose and is expressed in liver and pancreas (25).

HK2 comprises a mitochondria-targeting domain (25) that localizes the enzyme to the VDAC/adenine nucleotide translocase channel to promote the rapid phosphorylation of glucose by means of the ATP promptly translocated from the matrix to the cytoplasm (26). We observed that the absence of HK2 impairs mitochondrial oxygen consumption, similar to the conditions of ADP recycling inhibition. Furthermore, the opposed displacement of protons in the intermembrane space generates a cationic gradient in relation to the matrix that, in cells lacking HK2, increases the mitochondrial membrane potential. Because this condition forces the respiratory chain complexes into a reduced state, the chances of electron leaking increase, resulting in enhanced ROS and superoxide anion production. As shown in Fig. 5*D*, human keratinocytes expressing p63 rely on HK2 function to prevent mitochondrial oxidative stress. In this positive loop, the phosphorylation of glucose accelerates the mitochondrial electron flux, which in turn results in the proton gradient generating ATP. In rat brain mitochondria and cortical neurons, da-Silva et al. also reported the importance of HK2 subcellular localization in the proximity of VDAC in facilitating ADP recycling to the matrix and favoring a new cycle of oxidative phosphorylation (29). Based on our data and on published results (29), the HK2 antioxidant function resides in its capacity to contribute to ADP local recycling at the mitochondria (Fig. 5*C*).

Accumulation of oxidative damage is one of the mechanisms leading to cellular senescence, tissue degeneration, and age-related disorders (30–32). ΔNp63 has a crucial role in counteracting cellular senescence and organismal aging through its support of the proliferating potential of epithelial cells (5, 24, 33–37). Therefore, ΔNp63 could exert its antisenescence/antiaging functions, at least in part, through the activation of the HK2 gene, thus supporting mitochondria functions.

In cancers, HK2 is overexpressed as part of a general strategy to reprogram cancer cell metabolism toward aerobic glycolysis to sustain high proliferation rate (38–40). Several tumorigenic pathways enhance HK2 transcription, including p53 and p53 mutants in hepatoma cells (20); Pten and p53 deficiency, through activation of the AKT–mTORC1–4EBP1 axis and inhibition of miRNA143, respectively, in prostate cancer (41); and peroxisome proliferator-activated receptor-γ (PPARγ) in liver (42). These suggest that ΔNp63 could have a role in regulation of HK2 transcription downstream of AKT in cooperation with PPARγ, contributing to metabolic reprogramming. Interestingly, different responsive elements on HK2 gene, located upstream of the first exon and within the 15th intron, are used by PPARγ and ΔNp63, respectively.

Our results, although limited to one cell line, indicate that the ΔNp63–HK2 axis is also present in cancer cells, although further studies are needed to investigate its relationship with mitochondria, if any, as cancer cells present mitochondria dysfunction and rely on aerobic glycolysis. Nevertheless, the data shown suggest that ΔNp63 could participate in cancer metabolic reprogramming in human malignancies, such us head and neck squamous cell carcinomas, lung squamous cell carcinomas, and breast cancer (43–47), in which p63 is strongly implicated.

## Materials and Methods

**Cell Culture, Transfection, Infection, Western Blotting, and ChIP.** Human primary epidermal keratinocytes from neonatal foreskin [human epidermal keratinocytes from neonatal (HEKn); Life Technologies] were grown in EpiLife medium enriched with human keratinocyte growth supplement (Life Technologies) in dedicated rat tail collagen-type I (BD Biosciences)-coated equipment. siRNA transfections were performed according to the manufacturer's protocol provided with Lipofectamine RNAiMAX reagent (Invitrogen). siRNAs were purchased as smart pools of four oligos (Dharmacon/Thermo Scientific): Scramble (nontargeting pool; D-001810), sip63 (hTP63; L-003330), siHK1 (hHK1; L-006820), siHK2 (hHK2; L-006735), and sip53 (hTP53; L-003329). HEK 293E cells were grown in DMEM with 10% (vol/vol) FBS, 100 U penicillin, and 100 μg/mL streptomycin (Gibco/Invitrogen), and transfected by using the Effectene Transfection Reagent according to the manufacturer's protocol (Qiagen). HCC1937 cells were grown in RPMI 1640 with 10% (vol/vol) FBS and transfected as HEKs. Detailed information on RNA extraction, mtDNA extraction, quantitative real-time (RT)-PCR, FACS analysis, clonogenicity assay, ATP viability assay, EM, luciferase assay, retroviral vector generation, infection, ChIP, and Western blotting is provided in *SI Materials and Methods*.

**Seahorse Flux Analysis.** Oxidative phosphorylation and glycolysis flux were analyzed by measuring the OCR and lactic acid release or ECAR by using an XF24 XF analyzer (Seahorse Bioscience). Briefly, $1.5 \times 10^4$ Hekn cells were seeded into collagen-coated XF 24-well cell culture microplates (Seahorse Biosciences). The following day, the cells were transfected as described in *SI Materials and Methods*. Then, 48 h after transfection, the cells were washed three times with assay medium (DMEM 8.3 g/L, NaCl 30 mM, GlutaMax 2 mM, sodium pyruvate 1 mM, glucose 11.11 mM, phenol red, pH 7.4) and were allowed to equilibrate at 37 °C ($CO_2$-free). A disposable sensor cartridge, embedded with 24 pairs of fluorescent biosensors (oxygen and pH), was loaded with drugs in the dedicated delivery chambers. Injection of oligomycin was used to inhibit ATP synthesis, binding to complex V, and inducing the transition from the BR to the UR states. FCCP was used to increase the proton permeability of the mitochondrial membrane, leading to the maximal respiratory capacity (MR) state. Finally, rotenone was injected to inhibit NADH dehydrogenase (complex 1) and to block mitochondrial electron transport. Experiments were set up to achieve a treatment with the following concentrations: oligomycin 0.5 μM, FCCP 0.4 μM, and rotenone 1 μM. Acquisition and analysis were performed as described by Wu et al. (48), and, at the end of each assay, the number of viable cells was determined by a cell viability assay as previously described. The metabolic profile is provided in *SI Materials and Methods*.

**ACKNOWLEDGMENTS.** We thank Dr. Kelvin Cain for his assistance in the Seahorse experiments and Dr. A. Peschiaroli and A. Terrinoni for their scientific discussions. This work was mainly supported by Associazione Italiana per la Ricerca contro il Cancro (AIRC) Grant IG13387 (to E.C.) and partially supported by a Fondazione Roma malattie Non trasmissibili Cronico-Degenerative (NCD) Grant (to G.M.), Istituto Dermopatico dell'Immacolata/Istituto di Ricovero e Cura a Carattere Scientifico (R.F.), and the Medical Research Council (G.M.).

1. Blanpain C, Fuchs E (2006) Epidermal stem cells of the skin. *Annu Rev Cell Dev Biol* 22:339–373.
2. Bickenbach JR, Greer JM, Bundman DS, Rothnagel JA, Roop DR (1995) Loricrin expression is coordinated with other epidermal proteins and the appearance of lipid lamellar granules in development. *J Invest Dermatol* 104(3):405–410.
3. Byrne C, Tainsky M, Fuchs E (1994) Programming gene expression in developing epidermis. *Development* 120(9):2369–2383.
4. Candi E, Schmidt R, Melino G (2005) The cornified envelope: A model of cell death in the skin. *Nat Rev Mol Cell Biol* 6(4):328–340.
5. Candi E, et al. (2006) Differential roles of p63 isoforms in epidermal development: Selective genetic complementation in p63 null mice. *Cell Death Differ* 13(6):1037–1047.
6. Koster MI, et al. (2007) p63 induces key target genes required for epidermal morphogenesis. *Proc Natl Acad Sci USA* 104(9):3255–3260.

7. Koster MI, Kim S, Mills AA, DeMayo FJ, Roop DR (2004) p63 is the molecular switch for initiation of an epithelial stratification program. *Genes Dev* 18(2):126–131.
8. Truong AB, Kretz M, Ridky TW, Kimmel R, Khavari PA (2006) p63 regulates proliferation and differentiation of developmentally mature keratinocytes. *Genes Dev* 20(22):3185–3197.
9. Mills AA, et al. (1999) p63 is a p53 homologue required for limb and epidermal morphogenesis. *Nature* 398(6729):708–713.
10. Yang A, et al. (1999) p63 is essential for regenerative proliferation in limb, craniofacial and epithelial development. *Nature* 398(6729):714–718.
11. Yang A, Kaghad M, Caput D, McKeon F (2002) On the shoulders of giants: p63, p73 and the rise of p53. *Trends Genet* 18(2):90–95.
12. Yang A, McKeon F (2000) P63 and P73: P53 mimics, menaces and more. *Nat Rev Mol Cell Biol* 1(3):199–207.
13. Duijf PH, et al. (2002) Gain-of-function mutation in ADULT syndrome reveals the presence of a second transactivation domain in p63. *Hum Mol Genet* 11(7):799–804.
14. Yang A, et al. (1998) p63, a p53 homolog at 3q27-29, encodes multiple products with transactivating, death-inducing, and dominant-negative activities. *Mol Cell* 2(3): 305–316.
15. Romano RA, et al. (2012) ΔNp63 knockout mice reveal its indispensable role as a master regulator of epithelial development and differentiation. *Development* 139(4): 772–782.
16. Senoo M, Pinto F, Crum CP, McKeon F (2007) p63 Is essential for the proliferative potential of stem cells in stratified epithelia. *Cell* 129(3):523–536.
17. Su X, et al. (2012) TAp63 is a master transcriptional regulator of lipid and glucose metabolism. *Cell Metab* 16(4):511–525.
18. Berkers CR, Maddocks OD, Cheung EC, Mor I, Vousden KH (2013) Metabolic regulation by p53 family members. *Cell Metab* 18(5):617–633.
19. Gottlieb E, Vousden KH (2010) p53 regulation of metabolic pathways. *Cold Spring Harb Perspect Biol* 2(4):a001040.
20. Mathupala SP, Heese C, Pedersen PL (1997) Glucose catabolism in cancer cells. The type II hexokinase promoter contains functionally active response elements for the tumor suppressor p53. *J Biol Chem* 272(36):22776–22780.
21. Kouwenhoven EN, et al. (2010) Genome-wide profiling of p63 DNA-binding sites identifies an element that regulates gene expression during limb development in the 7q21 SHFM1 locus. *PLoS Genet* 6(8):e1001065.
22. Kouwenhoven EN, et al. (2015) Transcription factor p63 bookmarks and regulates dynamic enhancers during epidermal differentiation. *EMBO Rep* 16(7):863–878.
23. Giacobbe A, et al. (2015) p63 controls cell migration and invasion by transcriptional regulation of MTSS1. *Oncogene*, 10.1038/onc.2015.230.
24. Rivetti di Val Cervo P, et al. (2012) p63-microRNA feedback in keratinocyte senescence. *Proc Natl Acad Sci USA* 109(4):1133–1138.
25. Wilson JE (2003) Isozymes of mammalian hexokinase: Structure, subcellular localization and metabolic function. *J Exp Biol* 206(pt 12):2049–2057.
26. Robey RB, Hay N (2006) Mitochondrial hexokinases, novel mediators of the antiapoptotic effects of growth factors and Akt. *Oncogene* 25(34):4683–4696.
27. Gottlob K, et al. (2001) Inhibition of early apoptotic events by Akt/PKB is dependent on the first committed step of glycolysis and mitochondrial hexokinase. *Genes Dev* 15(11):1406–1418.
28. Majewski N, et al. (2004) Hexokinase-mitochondria interaction mediated by Akt is required to inhibit apoptosis in the presence or absence of Bax and Bak. *Mol Cell* 16(5):819–830.
29. da-Silva WS, et al. (2004) Mitochondrial bound hexokinase activity as a preventive antioxidant defense: Steady-state ADP formation as a regulatory mechanism of membrane potential and reactive oxygen species generation in mitochondria. *J Biol Chem* 279(38):39846–39855.
30. d'Adda di Fagagna F (2008) Living on a break: Cellular senescence as a DNA-damage response. *Nat Rev Cancer* 8(7):512–522.
31. Adams PD (2009) Healing and hurting: Molecular mechanisms, functions, and pathologies of cellular senescence. *Mol Cell* 36(1):2–14.
32. Rufini A, et al. (2012) TAp73 depletion accelerates aging through metabolic dysregulation. *Genes Dev* 26(18):2009–2014.
33. Paris M, Rouleau M, Pucéat M, Aberdam D (2012) Regulation of skin aging and heart development by TAp63. *Cell Death Differ* 19(2):186–193.
34. Sommer M, et al. (2006) DeltaNp63alpha overexpression induces downregulation of Sirt1 and an accelerated aging phenotype in the mouse. *Cell Cycle* 5(17):2005–2011.
35. Keyes WM, et al. (2005) p63 deficiency activates a program of cellular senescence and leads to accelerated aging. *Genes Dev* 19(17):1986–1999.
36. Viticchiè G, et al. (2012) MicroRNA-203 contributes to skin re-epithelialization. *Cell Death Dis* 3:e435.
37. Candi E, et al. (2007) DeltaNp63 regulates thymic development through enhanced expression of FgfR2 and Jag2. *Proc Natl Acad Sci USA* 104(29):11999–12004.
38. Vander Heiden MG, Cantley LC, Thompson CB (2009) Understanding the Warburg effect: The metabolic requirements of cell proliferation. *Science* 324(5930):1029–1033.
39. Patra KC, et al. (2013) Hexokinase 2 is required for tumor initiation and maintenance and its systemic deletion is therapeutic in mouse models of cancer. *Cancer Cell* 24(2): 213–228.
40. Peschiaroli A, et al. (2013) miR-143 regulates hexokinase 2 expression in cancer cells. *Oncogene* 32(6):797–802.
41. Wang L, et al. (2014) Hexokinase 2-mediated Warburg effect is required for PTEN- and p53-deficiency-driven prostate cancer growth. *Cell Reports* 8(5):1461–1474.
42. Panasyuk G, et al. (2012) PPARγ contributes to PKM2 and HK2 expression in fatty liver. *Nat Commun* 3:672.
43. Ramsey MR, et al. (2013) FGFR2 signaling underlies p63 oncogenic function in squamous cell carcinoma. *J Clin Invest* 123(8):3525–3538.
44. Ramsey MR, He L, Forster N, Ory B, Ellisen LW (2011) Physical association of HDAC1 and HDAC2 with p63 mediates transcriptional repression and tumor maintenance in squamous cell carcinoma. *Cancer Res* 71(13):4373–4379.
45. Piccolo S, Enzo E, Montagner M (2013) p63, Sharp1, and HIFs: Master regulators of metastasis in triple-negative breast cancer. *Cancer Res* 73(16):4978–4981.
46. Montagner M, et al. (2012) SHARP1 suppresses breast cancer metastasis by promoting degradation of hypoxia-inducible factors. *Nature* 487(7407):380–384.
47. Adorno M, et al. (2009) A Mutant-p53/Smad complex opposes p63 to empower TGFbeta-induced metastasis. *Cell* 137(1):87–98.
48. Wu M, et al. (2007) Multiparameter metabolic analysis reveals a close link between attenuated mitochondrial bioenergetic function and enhanced glycolysis dependency in human tumor cells. *Am J Physiol Cell Physiol* 292(1):C125–C136.
49. Tucci P, et al. (2013) Rapamycin regulates biochemical metabolites. *Cell Cycle* 12(15): 2454–2467.